

Anchorage Bond Strength of Glass Fibre Polymer Reinforced Concrete with Palm Kernel Shells as Partial Coarse Aggregate

ABSTRACT

Reinforced concrete with steel reinforcing bars have served most infrastructural needs such as buildings, roads, bridges, etc., but in recent years, the use of GFRP reinforcing bars in place of steel reinforcing bars in these structures cannot be overlooked as they offer advantages such as higher tensile strength, corrosion resistance, reduced weight and cost effectiveness compared to steel reinforcing bars. It is worthy of note that, several studies have been conducted on finding means of partially or fully replacing aggregates especially coarse aggregates in concrete and reinforced concrete for the purposes of producing lightweight concrete and reducing construction cost but the application of GFRP reinforcing bars in lightweight concrete such as PKSC requires further studies. The study focused on determining the anchorage bond strength of Glass Fibre Polymer reinforced concrete with PKS as partial coarse aggregate. Normal weight concrete mix ratio of 1:1.5:3 with water-cement ratio (w/c) of 0.5 and lightweight concrete with 10% of the volume of coarse aggregate replaced by PKS were used in double pull-out prismatic specimens of dimension 100mm x 100mm x 300mm for control and test specimens respectively, embedded with 12mm and 16mm diameter GFRP reinforcing bars at varying embedment lengths. Generally, the anchorage bond strength decreased with increasing (end-to-end) embedment length irrespective of the type of concrete mix and GFRP reinforcing bar size but further decrease were recorded for PKSC and an increase in GFRP reinforcing bar diameter resulted in a decrease in anchorage bond strength. Conversely, the PKSC specimens with 12mm and 16mm GFRP reinforcing bars and continuous (300mm) embedment length recorded the highest average anchorage bond strength values of 6.174N/mm² and 4.581N/mm² respectively. The 10% PKS replacement of concrete resulted in percentage average anchorage bond strength ranging between 75.5-97.9% of that of NWC. Splitting failure was observed for most of the specimens with longitudinal and transverse crack patterns developed after load application regardless of the size of GFRP reinforcing bar or concrete mix but the extent and visibility of the cracks formed reduced in specimens with continuous bar embedment.

Keywords: Reinforced Concrete; GFRP; Palm Kernel Shells; Anchorage Bond Strength; Partial Coarse Aggregate.

1. INTRODUCTION

Most structures are built using concrete which is a mixture of cementitious material, aggregates and water. Occasionally, an extra substance called an admixture is added to change certain properties for certain uses [1]. According to Chandra and Berntsson [2], studies have been carried out to find ways to partially or completely replace the conventional aggregates especially coarse aggregates in concrete in order to produce lightweight concrete, lower construction costs and reduce the rate of environmental degradation. Numerous research on the use of palm kernel shells (PKS) as LWA to replace NWA in structural elements and road construction in Southeast Asia and Africa have been conducted over the last 27 years [3]. The low tensile strength but high compressive strength of concrete requires the introduction of steel reinforcing bars which have high tensile strength in the tension zone of the concrete section to act compositely. Hence, the need for reinforced concrete. In steel reinforcement, corrosion is a chemical process that produces chemicals that damage the bond between steel reinforcing bars and concrete, decreasing bond strength and ultimately limiting the service life of reinforced concrete structures [4]. In nations like the US and Canada, this issue eventually results in a significant financial burden during routine maintenance, repairs and rehabilitation. In recent times, GFRP has become an alternative solution to the deterioration of civil infrastructures like bridge decks, tunnels, roads and other specialized concrete constructions due to its advantages over steel reinforcement including higher tensile strength, corrosion resistance, lighter weight and cost effectiveness [5, 32]. The most crucial prerequisite for reinforced concrete as a composite material is the efficacy of the bond strength between concrete and reinforcing bars [6]. The bond strength of the reinforcing bars in concrete can be ascertained in a few different ways. The ordinary pull-out test, push-out test, beam test and double pull-out test are a few of these tests. By measuring the force needed to remove the reinforcing bar that has been placed into the concrete specimen, the most popular test for determining the bond strength between concrete and steel reinforcing bar is the ordinary pull-out test which according to Bickley [7], was not thought of as a workable site method until the 1970s. However, the results of the ordinary pull-out test method, tend to be overestimated and does not depict the true bond strength of the concrete-reinforcing bar interface in the tensile zone as the concrete is subjected to compression while the steel bar is under tension [8]. Another pull-out test technique called the double pull-out test provides more precise bond strength results because it simulates the behavior of a beam tensile stress zone by putting tension on both the steel rebar and the concrete. Buabin et al. [8] studied the bond strength of steel reinforcing bars locally

milled from scrap metals in concrete prepared with Palm Kernel Shells as Coarse Aggregate by considering four concrete mixes with varying PKS contents in double pull-out prismatic specimens and embedded with 12mm and 16mm diameter steel reinforcing bars. PKS percentage replacement as well as bar type, size and geometry all impacted on anchorage bond strength. The anchorage bond strength was found to be between 2.84N/mm^2 and 10.13N/mm^2 . Odeyemi et al. [9] investigated the bond strength between high yield steel reinforcing bars and partially replaced Self Compacting PKS concrete in which 50% of the granite content of the concrete was substituted with palm kernel shells. It was determined that PKS could be safely used for partial replacement in SCC. Gupta et al. [10] studied the partial replacement of coarse aggregates with PKS at rates of 10%, 13%, 15%, 20%, and 25% in concrete by testing the compressive strength of 150 mm x 150 mm x 150 mm cubes which were cast with mix ratio, 1:1.5:3 by volume batch. Results showed that 10% partial replacement was optimum without compromising on the compressive strength of concrete. Alengaram et al. [11] concluded that, after examining previous research on the use of palm kernel shells (PKS) as lightweight aggregate (LWA), PKSC operates structurally and mechanically equivalent to normal weight concrete (NWC). Shahidi et al. [12] looked into the long-term performance of FRP and how sustained loading affected the bond between the concrete and the FRP bars. One type of GFRP, two types of Carbon FRP and conventional steel reinforcing bars were tested statically to failure and under sustained loads in pull-out specimens with different embedment lengths and the short-term bond strengths of FRP bars were found to be lower than those of steel. However, this study focuses on determining the anchorage bond strength of Glass Fibre Polymer reinforced concrete with PKS as partial coarse aggregate.

2. MATERIALS AND METHODS

2.1 Materials

The materials used for the study shown in (Fig. 1) included coarse aggregate (granite), fine aggregate, palm kernel shells used as partial replacement of coarse aggregate, ordinary Portland cement, water and GFRP reinforcing bars which are ribbed and sand-coated. The crushed granitic rock used as coarse aggregates had a maximum particle size of 20mm which exceeds and satisfies the minimum coarse aggregate size of 5mm specified by BS 882 [13]. Fine aggregate used was natural sand with maximum particle size of 4.75mm. The aggregates were air

dried and kept away from moisture in order to prevent bulking. Palm kernel shells used as partial replacement of coarse aggregates in test specimens were obtained from a local palm kernel oil factory and varied in sizes between 13.20mm and 2mm which is comparable to the study by Alengaram et al.[14]. Cement used was the ordinary Portland cement of weight 50kg and of grade 42.5R from the local market. Clean water devoid of contaminants was used. Glass Fibre Reinforcement Polymer (GFRP) reinforcing bars obtained from a local factory in Tema, Ghana, of actual diameters 12mm and 16mm respectively when measured with a Vernier caliper and expected minimum tensile strength of 758N/mm^2 as specified by the manufacturer were used in test specimens. Concrete mix ratio of 1:1.5:3 and water-cement ratio (w/c) of 0.5 were used for the normal weight concrete and 10% of the volume of coarse aggregate was substituted by PKS for the concrete with PKS as partial coarse aggregate replacement as determined by Gupta et al.[10] as the optimum PKS content without compromising on the compressive strength of concrete. The measurement of the gravel, sand, cement and PKS were by volume (m^3) and mixed with water measured in litres (ltr). Batching by volume was done because of the relatively low density of PKS compared to granite and would ensure accurate relative proportion of PKS in the mix. The palm kernel shells (PKS) were soaked in water for at least 20 minutes before batching since PKS has higher water absorption rate which has an effect on the workability of concrete and cement hydration [15]. The mixing was done manually on a clean surface.

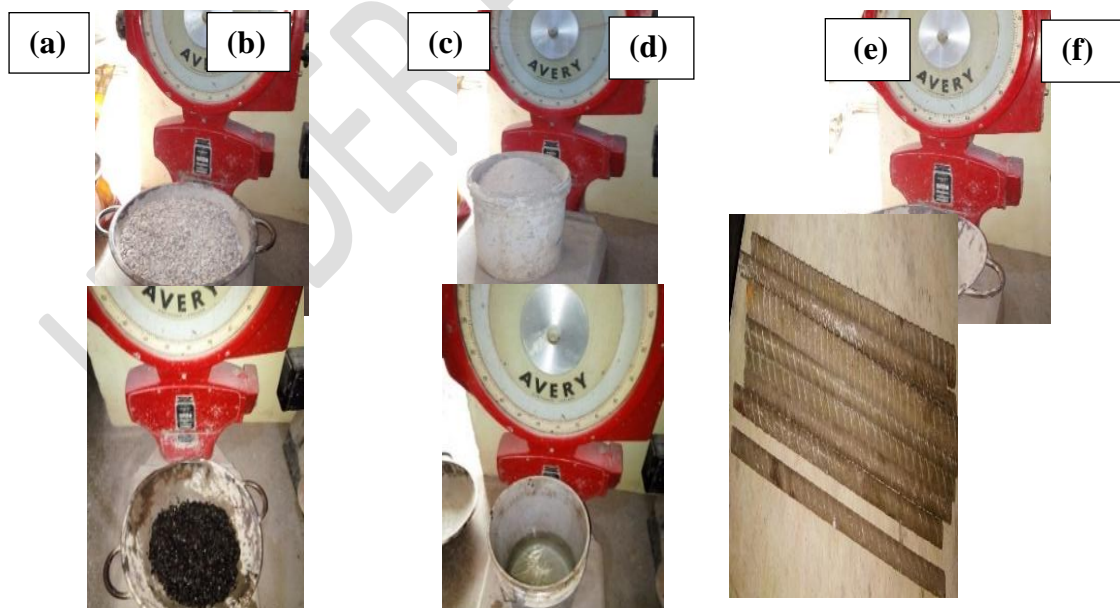


Fig.1: Materials: (a) gravel, (b) sand, (c) cement, (d) PKS soaked in water for 20mins, (e) water (f) cut GFRP bars.

2.2 Specimens

2.2.1 Concrete prism specimens

A total of forty-eight (48) test and control concrete prism specimens of dimension 100mm x 100mm x 300mm were cast for the anchorage bond or double pull-out test. Three (3) prisms each were with GFRP reinforcing bars of diameter 12mm and 16mm placed concentrically at varying embedment lengths of 300mm (continuous), 150mm (end-to-end), 125mm (end-to-end) and 100mm (end-to-end) embedment lengths for both test and control specimens respectively with a grip length of 100mm at both ends of each concrete prism as illustrated in (Fig.2). The notations of the test and control concrete prism specimens shown in Table 5, imply C-GF12 and C-GF16, represent the control specimens with NWC and GFRP reinforcing bars of diameters 12mm and 16mm respectively. S-GF12 and S-GF16 denote the test specimens with 10% PKS concrete and GFRP reinforcing bars of diameters 12mm and 16mm respectively. The ELS, EL150, EL125 and EL100 suffixes imply continuous, 150mm, 125mm and 100mm embedment length respectively.

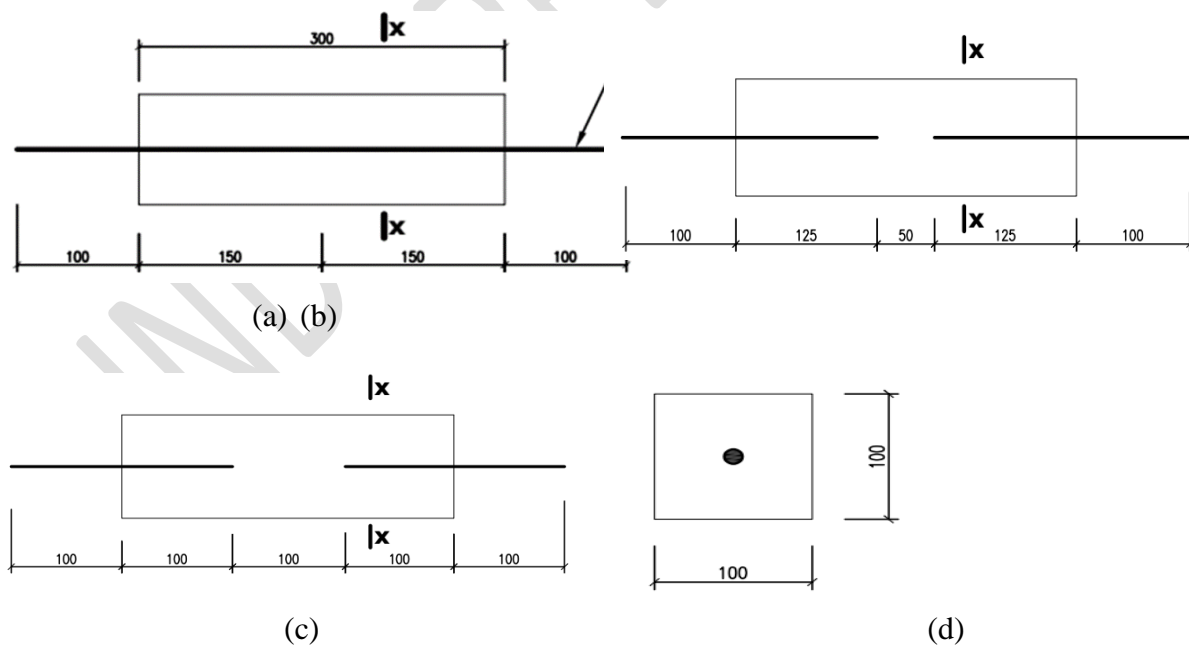


Fig. 2: Illustration of concrete prism specimens for double pull-out test:(a) with 150mm rebar embedment (b) with 125mm rebar embedment, (c) with 100mm rebar embedment, (d) section x-x

2.2.2 Concrete cube specimens

Nine (9) concrete cube specimens of dimension 150mm x 150mm x 150mm with 10% PKS as partial coarse aggregate replacement and nine (9) cubes with normal weight concrete were cast to determine their compressive strengths respectively. Three (3) cubes each of the two concrete mixes were used to determine the average compressive strengths after 7 days, 14 days, and 28 days respectively.

2.2.3 Concrete cylindrical specimens

Six (6) concrete cylindrical specimens of dimensions 150mm x 300mm as specified by BS EN 12390-6 [16] were used for the splitting tensile strength test. Three (3) specimens were with concrete with 10% PKS as partial coarse aggregate replacement and three (3) specimens with normal weight concrete. Table 4 shows the test specimens with 10% PKSC labelled S1, S2 and S3 and control specimens with NWC labelled C1, C2 and C3.

2.2.4 Tensile test specimens

Three (3) pieces of each of the GFRP reinforcing bars of actual diameters of 12mm and 16mm were measured with Vernier calipers and cut in lengths of 600mm to determine their tensile strength.

(a)

(b)



(c)

(d)



Fig. 3: Specimens: (a) Prism specimens, (b) Hardened prism specimen, (c) cylindrical specimens, (d) cube specimens

2.3 Test Procedure

2.3.1 Tensile test of GFRP

The tensile strength of the GFRP reinforcing bars was determined using the UTM in accordance with ASTM D7205 [17]. To prevent the premature failure at the grips due to stress concentrations at the anchorage points, adequate grip lengths of 150mm were used at the two ends of each specimen in order to allow failure to occur at the middle of the specimen during testing [18]. The two ends of each GFRP specimen were placed in steel tubes of lengths 150mm

and thickness of 3mm. The steel tubes had internal diameters of 16mm and 25mm to provide adequate space for the epoxy resin fill to ensure adequate bond with the GFRP reinforcing bar specimens of diameters 12mm and 16mm respectively. They were bonded together with a cementitious grout or epoxy resin surrounding the bar and allowed to dry for 2 days. The specimens were then placed in the upper and lower jaws of the UTM and an extensometer attached at the middle of the gauge length to measure the corresponding strains. Tensile force was applied gradually till the ideal failure mode of a GFRP reinforcing bar during tensile test which is the splitting of the bar ends [19]. The maximum tensile strength and corresponding strains of the GFRP reinforcing bar specimens were then recorded and the average determined. Figs. 4(a) and (b) respectively show the preparation of test specimens and the tensile strength test of GFRP reinforcing bar specimens using UTM.

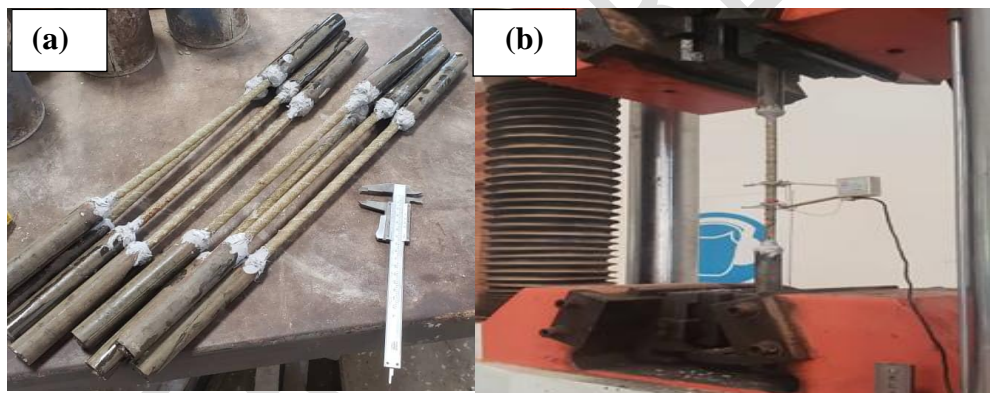


Fig. 4: GFRP reinforcing bar tensile test using UTM: (a) preparation of test specimens, (b) testing.

2.3.2 Anchorage bond test of GFRP

The anchorage bond or double pull-out test was conducted on the 28th day by fixing the two ends of the GFRP reinforcing bars embedded in the test and control concrete prism specimens firmly in position with the metallic wedges in both the upper and lower jaws of the UTM as shown in fig. 5 (a). The GFRP reinforcing bar grips at the ends of the prisms were not held during transportation and before testing in order to prevent any distortions or displacements. The two ends of the specimens were simultaneously pulled in tension until the embedded reinforcing bars

lost grip as the bond between the reinforcing bars and the surrounding concrete failed after exceeding the maximum force.

The anchorage bond strength is computed as; $F_b = \frac{P}{\pi dL}$(1)

Where; F_b = bond stress (N/mm²);

P = maximum applied load (N);

d= nominal diameter of rebar (mm);

L = embedment length of rebar (mm)

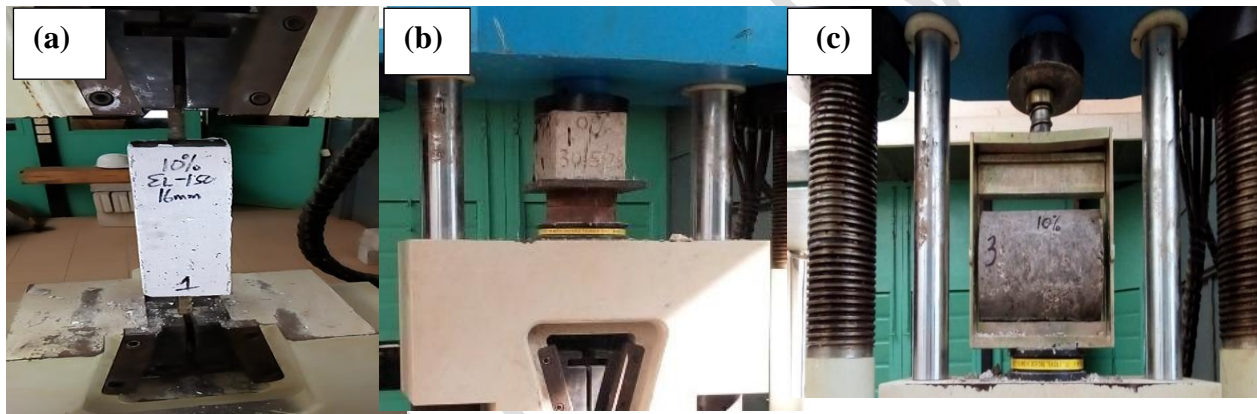


Fig. 5: Testing of specimens using UTM: (a) Anchorage bond strength (double pull-out) test, (b) compressive strength test, (c) splitting tensile strength test.

2.3.3 Concrete Compressive Strength Test

Compressive strength of the cured concrete cubes for each set at 7 days, 14 days and 28 days was determined in accordance with BS EN 12390-3 [20], using the UTM as shown in fig. 5 (b).

2.3.4 Concrete Split Cylinder Test

Splitting tensile strength was determined according to BS EN 12390-6[16]. The specimens were placed in a steel encasement of internal length 300mm and placed on the middle crosshead of the

UTM as shown in fig. 5 (c). Load was then applied to the specimens through the upper crosshead until splitting tensile failure of the concrete occurred.

The splitting tensile strength is computed as:

$$F_{\text{spt}} = \frac{2P}{\pi dL} \dots\dots\dots (2)$$

Where; F_{spt} = splitting tensile strength (N/mm²);

P = maximum applied load (N);

L = Length of test specimen (mm) and

d= diameter of specimen (mm)

3. RESULTS

3.1 Slump Test

The slump test result for the normal weight concrete ranged from 8mm to 45mm and that of the concrete with 10% PKS was 0mm which is comparable to the very low slump values (0–4 mm) reported by [21-24], indicating very low workability which can be attributed to the high porosity characteristics of PKS used as partial replacement of coarse aggregates. Significant amount of the water used for the batching might have been absorbed by the PKS and consequently, reduced the workability of PKSC.

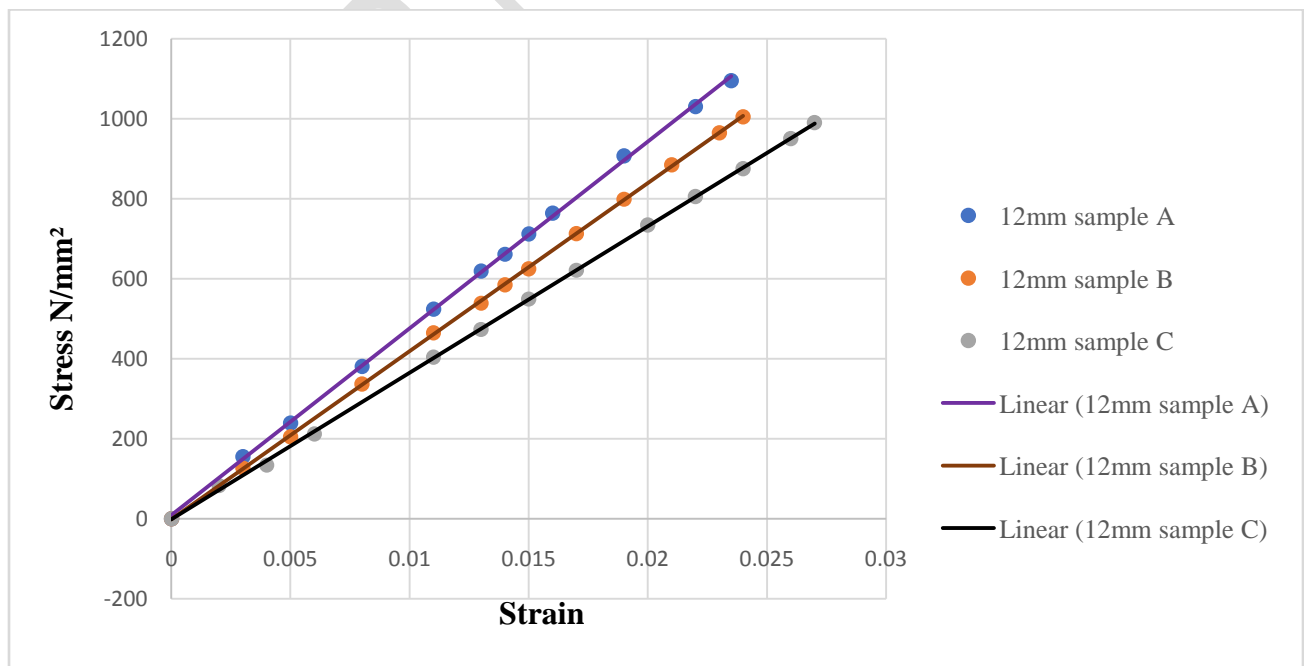
3.2 Tensile Strength of GFRP

Three samples labelled sample A, B and C respectively for each bar diameter were used for the test and an average tensile strength of 1030 N/mm² and maximum strain of 0.0248 were recorded for the 12mm GFRP reinforcing bar and an average tensile strength of 866 N/mm² and maximum strain of 0.028 for the 16mm GFRP reinforcing bar shown in Table 1. The average Young's modulus of elasticity recorded were 41.71GPa and 30.52GPa respectively for the 12mm and 16mm GFRP reinforcing bars. These values recorded exceeded the tensile strength and strain values provided by the local manufacturer. Figs. 6 (a) and (b) show the stress-strain curves for the GFRP reinforcing bars of diameter 12mm and 16mm used for the study respectively. Results

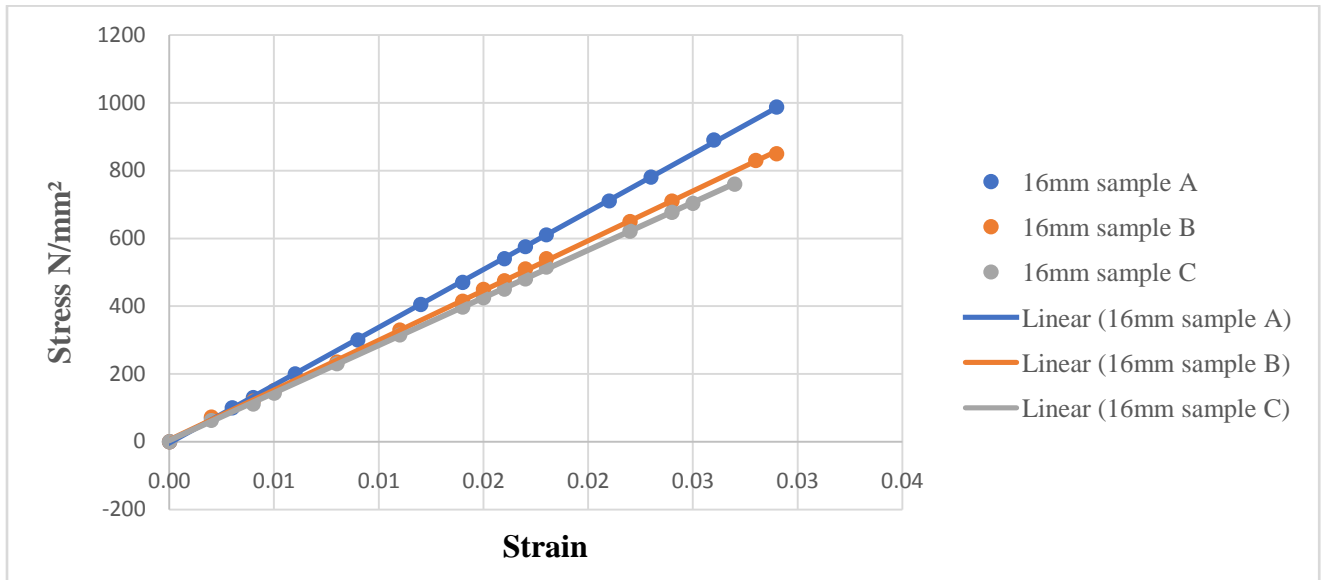
from the curves indicate an increase linearly throughout their deformations up to the maximum load where failure occurred suddenly. You et al. [25] reported similar stress-strain behaviour for GFRP reinforcing bar.

Table 1: Tensile strength test for GFRP reinforcing bars

SAMPLE	NOMINAL DIA., mm	ACTUAL DIA., mm	FORCE (P), N	MODULUS OF ELASTICITY (GPa)	TENSILE STRENGTH, N/mm ²	STRAIN
A	12	12	123844.50	46.43	1095	0.0235
B	12	12	113665.50	42.02	1005	0.0240
C	12	12	111969.00	36.68	990	0.0270
AVERAGE	12	12	116493.00	41.71	1030	0.0248
A	16	16	198446.22	34.10	987	0.0290
B	16	16	170901.00	29.36	850	0.0290
C	16	16	152805.60	28.09	760	0.0270
AVERAGE	16	16	174050.94	30.52	866	0.0280



(a)



(b)

Fig. 6: Stress-strain curve for tested: (a) 12mm diameter GFRP reinforcing bars, (b) 16mm diameter GFRP reinforcing bars

3.3 Concrete Compressive Strength

Cube specimens with NWC had average compressive strengths of 18.07 N/mm², 20.23 N/mm² and 22.25 N/mm² after 7 days, 14 days and 28 days respectively and those with 10% PKS as partial coarse aggregate replacement had average compressive strengths of 10.37 N/mm², 14.36 N/mm² and 15.79 N/mm² after 7 days, 14 days and 28 days respectively indicating a 29% reduction in the 28 days compressive strength for the PKSC. The average compressive strengths of the two concrete mixes are plotted against age in (Fig. 7) and the average 28 days compressive strength of both concrete mixes are shown in Tables 2 and 3 respectively.

3.4 Concrete Splitting Tensile Strength

The average splitting tensile strength value obtained for the NWC using Equation (2) was 2.76 N/mm² and 1.94 N/mm² for concrete with 10% PKS as partial coarse aggregate replacement which

indicates a 29.71% reduction and almost comparable to the values (2.0-2.4N/mm²) obtained by [23, 26, 40]. Table 4 and Fig. 8 show the results of splitting tensile strength test of the NWC and PKSC after 28 days.

Table 2: 28 days compressive strength for 10% PKS concrete

28 DAYS TEST			
Sample	1	2	3
Mass (kg)	7.055	7.117	8.135
Compressive Strength (N/mm ²)	12.79	15.54	19.04
Average Compressive Strength (N/mm ²)	15.79		

Table 3: 28 days compressive strength for normal weight concrete

28 DAYS TEST			
Sample	1	2	3
Mass (kg)	7.944	8.124	7.895
Compressive Strength (N/mm ²)	22.11	23.32	21.34
Average Compressive Strength (N/mm ²)	22.25		

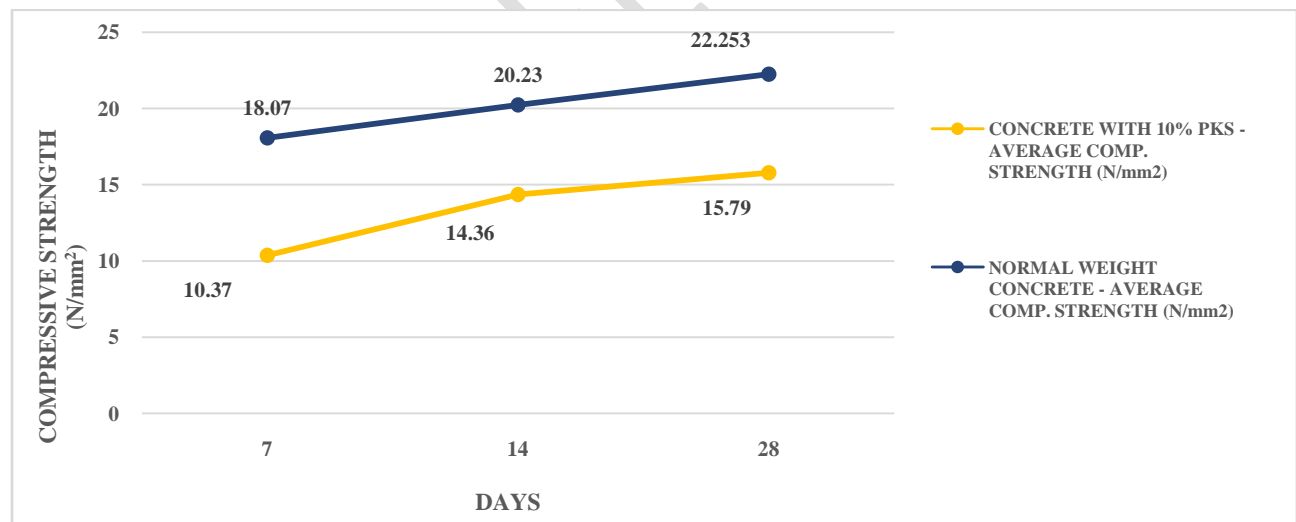


Figure 7: Average compressive strength versus days

Table 4: Splitting tensile strength test

S/No.	SAMPLE	LOAD, P (N)	SPLITTING TENSILE STRESS (N/mm ²)	AVE. SPLITTING TENSILE STRESS (N/mm ²)
1	C1	221704.00	3.14	2.76
2	C2	183073.00	2.59	
3	C3	179542.00	2.54	
	AVERAGE	194773.00	2.76	
4	S1	124849.00	1.77	1.94
5	S2	152155.00	2.15	
6	S3	134779.00	1.91	
	AVERAGE	137261.00	1.94	

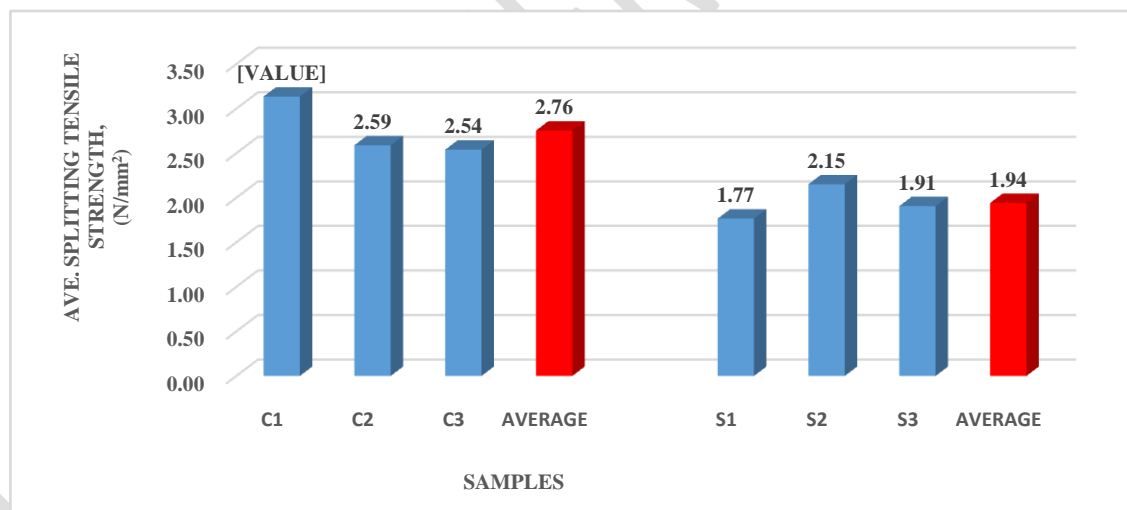


Figure 8: Average splitting tensile strength of normal weight and PKS concrete

3.5 Anchorage Bond Strength

The average anchorage bond strength were computed with Equation (1) and values recorded for the test and control prism specimens with GFRP bars of diameters 12mm and 16mm and various embedment lengths are shown in Table 5 and Fig. 9. The values for the specimens with 300mm

(continuous) embedment were obtained by considering half of the length (150mm) based on a study by Tang [38] which indicates that, bond stress–slip relationship varied with the position of the reinforcing bar and the closer the stress was to the center of the specimen, the steeper the curve became and the more the bond stiffness increased which was determined by considering half of the length of the specimen. Therefore, the average anchorage bond strength obtained for the test and control specimens with 12mm GFRP bars and 300mm (continuous) embedment were respectively 6.174N/mm^2 and 6.306N/mm^2 . The results obtained for the test and control specimens with 16mm GFRP bars and 300mm (continuous) embedment were respectively 4.581N/mm^2 and 5.584N/mm^2 . Average anchorage bond strength values of 3.051N/mm^2 and 3.558N/mm^2 were respectively recorded for the test and control specimens with 12mm GFRP bars and 150mm (end-to-end) embedment, 2.899N/mm^2 and 3.198N/mm^2 were respectively for the test and control specimens with 16mm GFRP bars and 150mm (end-to-end) embedment, 4.464N/mm^2 and 5.287N/mm^2 were respectively for the average anchorage bond strength for the test and control specimens with 12mm GFRP bars and 125mm (end-to-end) embedment, 3.087N/mm^2 and 3.259N/mm^2 were respectively recorded for the test and control specimens with 16mm GFRP bars and 125mm (end-to-end) embedment, 4.684N/mm^2 and 5.592N/mm^2 were respectively recorded for the test and control specimens with 12mm GFRP bars and 125mm (end-to-end) embedment and lastly, 3.558N/mm^2 and 4.712N/mm^2 for the test and control specimens with 16mm GFRP bars and 125mm (end-to-end) embedment.

Table 5: Average anchorage bond strength for test and control prism specimens with GFRP reinforcing bars at varying embedment lengths.

<u>SAMPLE</u>	<u>ACTUAL DIAMETER, (mm)</u>	<u>EMBEDMENT LENGTH (mm)</u>	<u>AVE. ANCHORAGE BOND STRESS (N/mm²)</u>	<u>% AVE. ANCHORAGE BOND STRESS OF NWC</u>
C-GF12-ELS	12	300 (continuous)	6.306	97.901
S-GF12-ELS	12	300 (continuous)	6.174	
C-GF16-ELS	16	300 (continuous)	5.584	
S-GF16-ELS	16	300 (continuous)	4.581	
C-GF12-EL150	12	150 (end-to-end)	3.558	85.750
S-GF12-EL150	12	150 (end-to-end)	3.051	
C-GF16-EL150	16	150 (end-to-end)	3.198	
S-GF16-EL150	16	150 (end-to-end)	2.899	
C-GF12-EL125	12	125 (end-to-end)	5.287	84.424
S-GF12-EL125	12	125 (end-to-end)	4.464	
C-GF16-EL125	16	125 (end-to-end)	3.259	

S-GF16-EL125	16	125 (end-to-end)	3.087	94.720
C-GF12-EL100	12	100 (end-to-end)	5.592	83.759
S-GF12-EL100	12	100 (end-to-end)	4.684	
C-GF16-EL100	16	100 (end-to-end)	4.712	
S-GF16-EL100	16	100 (end-to-end)	3.558	

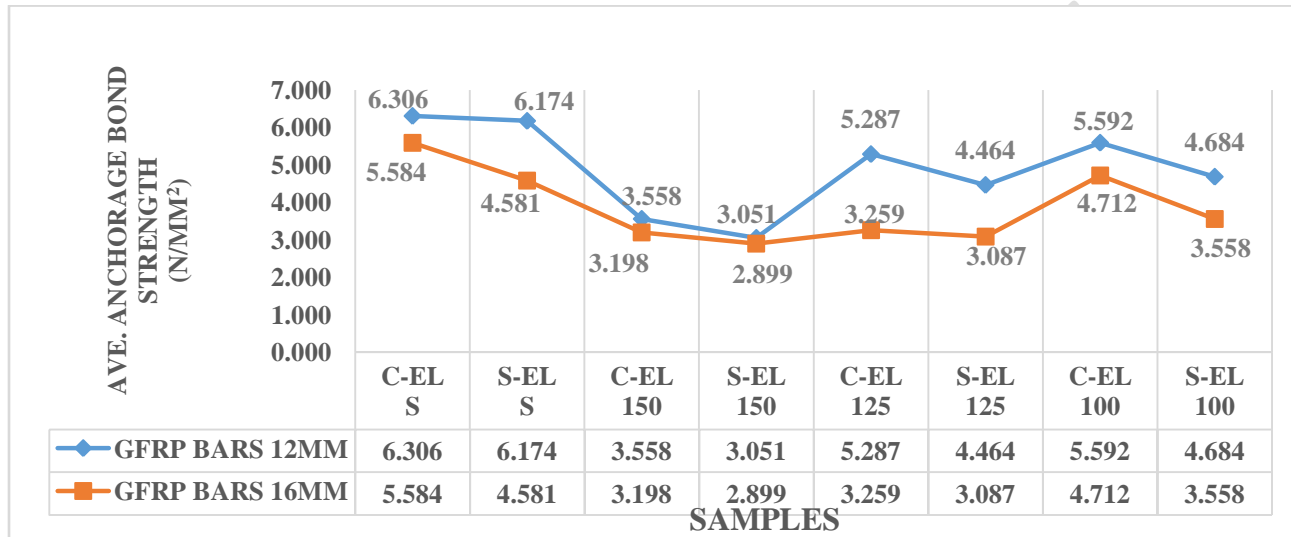
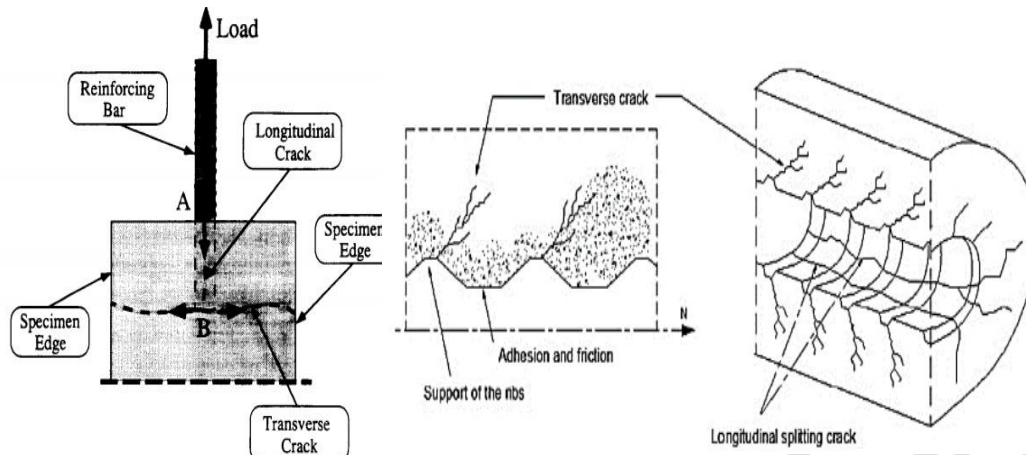


Figure 9: Comparison of the average anchorage bond strength of control and test prism specimens with GFRP reinforcing bars of diameter 12mm and 16mm at varying embedment lengths.



Figure 10: Tested double pull-out prism specimens with GFRP rebars.



(a) Krstulovic-Opara et al. [36] (b) Sulaiman et al. [37]

Figure 11: Crack Pattern Propagation

4. EFFECT OF EMBEDMENT LENGTH ON THE ANCHORAGE BOND STRENGTH

Generally, the average anchorage bond strength for all the test and control specimens with end-to-end embedment of GFRP reinforcing bars increased with decreasing embedment length. However, the average anchorage bond strength values of the test specimens with 10% PKS concrete remained lower compared to that of the control specimens with NWC and GFRP reinforcing bars of diameter 12mm and 16mm as shown in Table 5 and Fig. 9. Increase in bond strength with decreasing embedment lengths were also observed by [27-29] and can be attributed to the gradual transfer of the bond stress during the pull-out test from the loaded end to the free end which results in a nonlinear stress distribution of the bond stress along the embedment length [29,30]. Conversely, the specimens with 300mm (continuous) embedment recorded the highest average anchorage bond strength values of 6.174N/mm^2 and 6.306N/mm^2 respectively for 12mm GFRP reinforcing bars in the test and control specimens and 4.581N/mm^2 and 5.584N/mm^2 respectively for 16mm GFRP reinforcing bars in the test and control specimens which can be attributed to the study by Tang [38] which reported that the maximum value on the stress distribution curve mainly occurred at or near the central anchored point, whereas the minimum value occurred at the loaded end due to the symmetry.

5. EFFECT OF BAR SIZE ON THE ANCHORAGE BOND STRENGTH

Generally, Table 5 and Fig.9 show greater anchorage bond strength for specimens with GFRP reinforcing bars of 12mm diameter compared to 16mm. Previous studies by Hao et al. [31] and Patil and Manjunatha [33] show a reduction in bond strength values for larger GFRP reinforcing bar diameters.

6. EFFECT OF PKS CONTENT ON THE ANCHORAGE BOND STRENGTH

The 10% PKS replacement caused a reduction in the compressive strength by 29% and 29.71% reduction in splitting tensile strength as shown in Figures 7 and 8 respectively and consequently, a reduction in the anchorage bond strength as shown in Table 5 and Fig. 9. These observations are similar to previous studies by Olanipekun et al. [39] who studied the mechanical properties of PKS using 1:1:2 and 1:2:4 mix ratios with 0%, 25%, 50%, 75% and 100% replacement with PKS and reported a reduction in the compressive strength with the increasing PKS content and Alengaram et al. [40] compared the bond properties of PKSC with NWC and reported that the bond strength of PKSC was 86% of that of NWC which is in the range of (75.5-97.9%) indicated in Table 5 of this study recorded as the percentage bond strength of the NWC for the 10% PKSC.

7. FAILURE MODE AND CRACK PATTERNS

Most of the specimens shown in Fig. 10 developed longitudinal cracks that propagated from the point (A) illustrated in Figs.11(a) and (b) as the load was applied and towards the embedded bar end at point (B). At point (B), opening of the existing crack continues and is accompanied by the development of a transverse crack extended from point (B) toward the specimen edges. The specimen failed when the transverse crack reached the specimen edges. This pattern was noted in earlier research by Goto [34] and Diab et al. [35], where splitting bond failure is extremely sudden and brittle due to the rapid production of longitudinal splitting cracks. Development of the transverse crack can be attributed to the matrix-tension failure through the net concrete section at the point of high concrete tensile stress concentration developed at the reinforcing bar

end where there is a loss of most of its bond [36]. Similar crack patterns were observed for both test and control specimens regardless of the size of GFRP reinforcing bar and concrete mix. However, a few specimens had no visible cracks after testing. Cracks on the specimens with continuous or straight GFRP reinforcing bar embedment of 300mm had less visible cracks compared with specimens with discontinuous embedment lengths of 150mm, 125mm and 100mm which had similar and very visible cracks.

8. CONCLUSIONS

The following conclusions are drawn from the test results:

- i. Significant amount of water was absorbed by the PKS which subsequently reduced the workability of the concrete with PKS as partial coarse aggregate replacement compared with the granite in the NWC.
- ii. The 28 days compressive strength of the 10% PKSC was 15.79N/mm^2 which indicates a 29% reduction compared with the NWC and consequently contributed to the reduction in the anchorage bond strength.
- iii. The splitting tensile strength of 10% PKSC decreased by 29.71% compared with the NWC and consequently contributed to the reduction in the anchorage bond strength.
- iv. The 10% PKS replacement of concrete resulted in percentage average anchorage bond strength ranging between 75.5-97.9% of that of NWC.
- v. Anchorage bond strength decreased with increasing (end-to-end) embedment length irrespective of the type of concrete mix and GFRP reinforcing bar size but further decrease were recorded for PKSC. Conversely, the PKSC specimens with 12mm and 16mm GFRP reinforcing bars and continuous embedment length recorded the highest average anchorage bond strength values of 6.174N/mm^2 and 4.581N/mm^2 respectively.
- vi. Comparatively, the anchorage bond strength decreased with increase in GFRP reinforcing bar diameter.
- vii. Splitting failure was observed for most of the specimens with longitudinal and transverse crack patterns developing after load application regardless of the size of GFRP reinforcing

bar or concrete mix but the extent and visibility of the cracks formed reduced in specimens with continuous bar embedment.

REFERENCES

- [1] Jackson N., Dhir R. K. (1996). *Civil Engineering Materials* (5th Edition). Palgrave. pg. 163. ISBN 978-0-333-63683-1
- [2] Chandra, S., Berntsson, L. (2003). *Lightweight Aggregate Concrete – Science, Technology and Applications*. Norwich, New York: William Andrew Publishing.
- [3] Teo, D.C.L., Mannan, M. A., Kurian, V. J., Ganapathy C. (2007). Lightweight concrete made from oil palm shell (OPS): structural bond and durability properties. *Building and Environment*, 42 (7):2614–21.
- [4] Koch G. H., Brongers M. P., Thompson N.G., Virmani Y. P., Payer J. H. (2002). Corrosion cost and preventive strategies in the United States.
- [5] Nanni, A., De Luca, A., Zadeh, H. J. (2014). *Reinforced Concrete with FRP Bars: Mechanics and Design*. CRC Press, Taylor and Francis Group, LLC.
- [6] Lemnitzer, L., Schrödera, S., Lindorfa, A., Curbach, M. (2009). Bond behaviour between reinforcing steel and concrete under multiaxial loading conditions in concrete containments. 20th International Conference on Structural Mechanics in Reactor Technology (SMiRT 20) Espoo, Finland, August 9-14, 2009 SMiRT 20-Division II, Paper 1734.
- [7] Bickley, J. A. (2009). A Brief History of Pullout Testing with Particular Reference to Canada-A Personal Journey Symposium Paper Vo. 261, Pg. 277-286 DOI: 10.14359/51663217
- [8] Buabin, T. K., Kankam, C. K., Meisuh, B. K. (2017). Bond Strength of Reinforcing Steel Bars locally milled from Scrap Metals in Concrete prepared with Palm Kernel Shell as Coarse Aggregate. *International Journal of Engineering and Technical Research (IJETR)* ISSN: 2321-0869 (O) 2454-4698 (P) Volume-7, Issue-11.

- [9] Odeyemi, S.O., Abdulwahab, R., Abdulsalama, A.A., Anifowose, M.A. (2019). Bond and Flexural Strength Characteristics of Partially Replaced Self-Compacting Palm Kernel Shell Concrete. *Malaysian Journal of Civil Engineering*, 31, 1–7.
- [10] Gupta, S. K., Singh, S., Ahmad, S., Ambedkar, L. (2017). Partial Replacement of Coarse Aggregate with Palm Kernel Shell in Concrete, *International Journal of Engineering Research & Technology (IJERT) ISSN: 2278-0181 Vol. 6 Issue 04, April-2017*.
- [11] Alengaram U. J., Muhit B. A., Jumaat M. Z. (2012). Utilization of oil palm kernel shell as lightweight aggregate in concrete – A review. *Construction and Building Materials* 38 (2013), pg. 161–172.
- [12] Shahidi, F., Wegner, L., Sparling, B. (2011). Investigation of bond between fibre-reinforced polymer bars and concrete under sustained loads. *Canadian Journal of Civil Engineering*. 33. 1426-1437. 10.1139/106-070.
- [13] BS 882:1992, Specification for aggregates from natural sources for concrete. British Standard Institution, 2002.
- [14] Alengaram, U. J., Mahmud, H., Jumaat, M. Z., Shirazi, S. M. (2010). Effect of aggregate size and proportion on strength properties of palm kernel shell concrete. *International Journal of the Physical Sciences* 2010; 5(12):1848–1856.
- [15] Teo, D.C.L., Mannan, M. A., Kurian, V. J. (2006). Structural concrete using oil palm shell (OPS) as lightweight aggregate. *Turkish Journal of Engineering and Environmental Sciences*, 30(4):1–7.
- [16] BS EN 12390-6 (2009). Testing hardened concrete-Part 4: Tensile splitting strength of test specimens. British Standard Institution, London 2009.
- [17] ASTM D7205 (2006). Standard Test Method for Tensile Properties of Fiber Reinforced Polymer Matrix Composite Bars. ASTM Committee D30, 2006.
- [18] ACI 440.1R-15, Guide for the Design and Construction of Structural Concrete Reinforced with Fiber-Reinforced Polymer Bars, ACI Committee 440, 2015.

- [19] Kocaoz, S., Samaranayake, V., Nanni, A. (2005). Tensile characterization of glass FRP bars. *Composites Part B: Engineering* 2005; 36(2):127-134.
- [20] BS EN 12390-3 (2009). Testing hardened concrete-Part 3: Compressive strength of test specimens. British Standard Institution, London 2009.
- [21] Mannan, M. A., Ganapathy, C. (2001). Long-term strengths of concrete with oil palm shell as coarse aggregate. *Cement and Concrete Research* 2001; 31(9):1319-1321.
- [22] Okpala, D.C. (1990). Palm kernel shell as a lightweight aggregate in concrete. *Building and Environment*. 25(4):291–296.
- [23] Okafor, F. O. (1988). Palm kernel shell as a lightweight aggregate for concrete. *Cement and Concrete Research*. 18(6):901–910.
- [24] Ali, A. A. A. (1984). Basic strength properties of lightweight concrete using agricultural wastes as aggregates. In: *International Conference on Low Cost Housing for Developing Countries*. 12-17 Nov. 1984. Roorkee India. (pp. 143-146).
- [25] You, Y.J., Park, K.T., Seo, D.W., Hwang, J.H. (2015). Tensile Strength of GFRP Reinforcing Bars with Hollow Section. *Advances in Materials Science and Engineering*, Vol. 2015, Article ID 621546.
- [26] Teo, D.C.L., Mannan, M. A., Kurian, V. J. (2006). Flexural behaviour of reinforced lightweight concrete beams made with oil palm shell (OPS). *Journal of Advanced Concrete Technology*, 4 (3):1–10.
- [27] Esraa, K. J. (2017). Experimental Study on Anchorage Bond in High Strength Reinforced Concrete Beams. *International Journal of Civil Engineering and Technology*, 8(1), 2017, pp. 63–71.
- [28] Ferguson, P.M., Thompson, J.N. (1965). Development Length for Large High Strength Reinforcing Bars. *Journal of the American Concrete Institute*, January 1965, pp 71-91.
- [29] Di, B., Wang, J., Li, H., Zheng, J., Zheng, Y., Song, G. (2019). Investigation of Bonding Behavior of FRP and Steel Bars in Self-Compacting Concrete Structures Using Acoustic Emission Method. *Sensors (Basel)*. 2019 Jan 4; 19(1):159.doi:10.3390/s19010159.

- [30] Huang, H., Yuan, Y. J., Zhang, W., Hao, R. Q., Zeng, J. (2020). Bond properties between GFRP bars and hybrid fiber-reinforced concrete containing three types of artificial fibers. *Construction Building Materials*. 250, 18. doi:10.1016/j.conbuildmat.2020.118857
- [31] Hao, Q.D., Wang, Y.L., Zhang, Z.C., Ou, J.P. (2007). Bond Strength Improvement of GFRP Rebars with Different Rib Geometries. *Journal of Zhejiang University-Science A: Applied Physics & Engineering*. 8. 1356–1365.
- [32] Patil, G.S., Adakurkar, K., Chougule, V., Naik, S., Shitole, K., Kokate, A. (2021). Applications of Glass Fibre Reinforced Polymer (GFRP) in Concrete Structures – A review. *International Journal of Research Publication and Reviews Vol. 2, No. 10*, pp. 214-216.
- [33] Patil, S.B., Manjunatha G. (2020). Experimental study on bond strength of GFRP bars. *Mater Today: Proc 2020;21:1044–9*.
- [34] Goto, Y. (1971). Cracks formed in concrete around deformed tension bars. *ACI Journal, Proceedings*, 68 (1971) 244-51
- [35] Diab, A. M., Elyamany, H. E., Hussein, M.A., Ashy, H. M. A. (2014). Bond behavior and assessment of design ultimate bond stress of normal and high strength concrete, *Alexandria Engineering Journal 2014; 53(2):355–371*.
- [36] Krstulovic-Opara, N., Watson, K. A., LaFave J. M. (1993). Effect of Increased Tensile Strength and Toughness on Reinforcing-Bar Bond Behaviour. *Cement and Concrete Composites* 16 (1994) 129-141.
- [37] Sulaiman, M.F., Ma, C.K., Apandi, N. M., Chin, S., Awang, A. Z., Mansur, S. A., Omar W. (2017). A Review on Bond and Anchorage of Confined High-strength Concrete. *Structures*, 2017 (11), pp. 97-109.
- [38] Tang, C.-W (2021). Modeling Uniaxial Bond Stress–Slip Behavior of Reinforcing Bars Embedded in Concrete with Different Strengths. *Materials* **2021**, *14*, 783. <https://doi.org/10.3390/ma14040783>
- [39] Olanipekun, E. A., Olusola, K. O., Ata, O. (2006). A Comparative Study of Concrete Properties using Coconut Shell and Palm Kernel Shell as Coarse aggregates. *Building and Environment* 2006; 41 (3):297–301.

[40] Alengaram, U. J., Mahmud, H., Jumaat, M. Z. (2010). Comparison of mechanical and bond properties of oil palm kernel shell concrete with normal weight concrete. *Int JPhys Sci* 2010;5(8):1231–9.

UNDER PEER REVIEW